59th ILMENAU SCIENTIFIC COLLOQUIUM
Technische Universität Ilmenau, 11 – 15 September 2017
URN: urn:nbn:de:gbv:ilm1-2017iwk-102:0

EVALUATION STRATEGY OF SPHEROIDAL DISTORTION FOR MICRO-SPHERE BASED ON WHISPERING GALLERY MODE RESONANCE

K. Hayashi[1], B. Chu[2], Z. Zhao[1], M. Michihata[3], K. Takamasu[1], S. Takahashi[3]

[1]Department of Precision Engineering, The University of Tokyo, Japan
[2]Department of Advanced Interdisciplinary Studies, The University of Tokyo, Japan
[3]Research Center for Advanced Science and Technology, The University of Tokyo, Japan

ABSTRACT

The demand for measuring the diameter of the spherical object, which is used for the CMM stylus, for example, is now rising and its measurement error is desired to be less than several 10 nm for the spherical object whose size is around 100 μm. To achieve this, the measurement method based on WGM resonance is remarkable. But as long as we rely on this method, the model of the object must be a perfect sphere, and this assumption should not always be valid. Practically, a measured sphere has the rotational symmetry so that it suffices to evaluate the spheroidal distortion to know the macro-distortion. According to this motivation, we proposed the new measurement method to appreciate the degree of distortion for the object based on WGM resonance. Degeneracy for azimuthal direction disappears if the object distorted spheroidal-like. Hence, we can measure the interval between the resonant wavelengths for different azimuthal mode number and evaluate the degree of spheroidal distortion.

Index Terms - Whispering Gallery Mode, resonance, diameter measurement, spheroidal distortion

1. INTRODUCTION

In one exemplary aspect, micro-CMM (Coordinate Measuring Machine) has a micro sphere on tip of its probe. If the size of this probe sphere has an ambiguity, this affects the measurement precision of micro-CMM for un-ignorable degrees. Consequently, the absolute evaluation of the size of a micro sphere is necessary in metrological field. Practically, measuring a micro sphere whose diameter is around 100 μm with around 10 nm precision is required. To achieve this precision, we focus on the measurement method using the resonance phenomena called "whispering Gallery Mode resonance"[1]. This resonance is one of resonance phenomena of light wave, which occurs when the projected object has a spherical structure. We expect this method to achieve the desired measurement precision in non-contact and non-destructive way.

However, when we measure the object sphere by using Whispering Gallery Mode resonance, we assume that the model is a perfect sphere. In fact, this assumption usually fails from an experimental point of view. Many spheres have some distortion, i.e. the measured sphere is not always a perfect sphere. For example, measured sphere is sometimes chipped or dazzling in micro scale, or it is flatly crushed or elongated in macro scale. In this article, by focusing on the spheroidal distortion among above kinds of distortion, we consider the case that the object sphere is not necessarily a perfect sphere to confirm the validity of the measurement method based on the Whispering Gallery Mode resonance.

For instance, it is possible to manufacture micro spheres based on an aggregation property of the material, namely, by using surface tension of micro particles. Hence, it suffices to have a good measurement method that is suitable for measuring particles having rotational symmetry.

From this point of view, we expand the theoretical particle model from a perfect sphere to a spheroid and propose a new method to evaluate the spheroidal distortion of the measured object in this article.

2. SPHERE DIAMETER MEASUREMENT BASED ON WGM RESONANCE

2.1 Whispering Gallery Mode Resonance

First, we introduce what Whispering Gallery Mode (WGM) resonance is. When the incident light wave is radiated into a sphere, there are some oscillation modes such that the light wave strongly resonates. This situation is described as that the incident light wave cirques around a surface of a sphere like **Fig.1**, which causes a strong resonance and scattering simultaneously. This resonance is called Whispering Gallery Mode (WGM) resonance and each oscillation mode is one of Whispering Gallery modes.

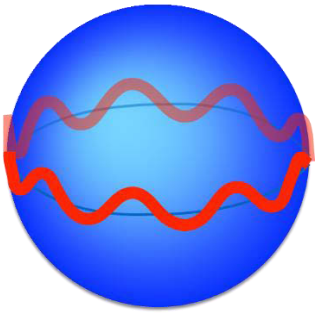

Fig.1 Whispering Gallery Mode (WGM) resonance

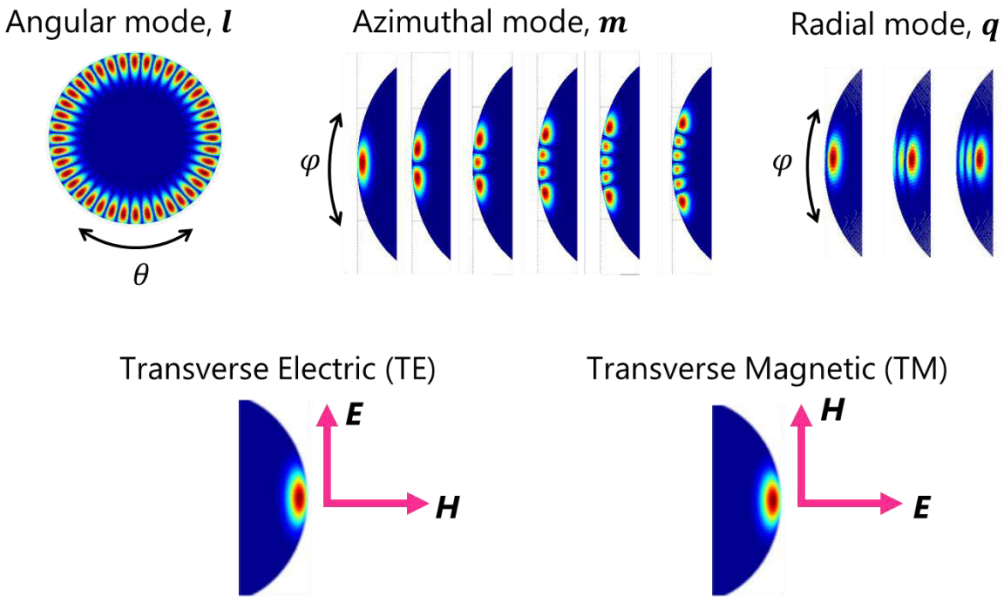

Fig.2 Mode numbers of WGM and modes about polarization (TE / TM)

Above Whispering Gallery Resonance is classified by the way for which the light wave propagates in a sphere. Namely, WG modes have three kinds: angular mode, azimuthal mode, and radial mode. These modes characterize how the light wave propagate in a sphere, and angular mode, azimuthal mode, and radial mode are identified by integers l, m, q, respectively. In addition, two kinds of modes about the polarization of the light wave exist: transverse electric (TE) mode and transverse magnetic (TM) mode. The oscillation direction of electric field is

perpendicular to the tangential plane in TE mode, whereas is parallel to the tangential plane in TM mode. **Fig.2** shows conceptual description of each mode.

2.2 Theoretical background - interaction between a spherical particle and light wave

To determinate WGM resonant wavelengths for sphere with arbitrary size, solving the problem about interaction between the particle and light wave is necessary. In other words, we have to solve the Maxwell's equations for the coordinate system that is appropriate for the shape of the measured object. In this case, when the measured object is assumed as a perfect sphere, solving the following Maxwell's equation in a spherical coordinate system enables us to know the WGM resonant wavelengths corresponding to the condition of each model and incident light wave in advance.

The Maxwell's equations in vacuum are given as following.

$$\begin{cases} \boldsymbol{\nabla} \cdot \boldsymbol{E} = 0 \\ \boldsymbol{\nabla} \cdot \boldsymbol{H} = 0 \\ \boldsymbol{\nabla} \times \boldsymbol{E} = -\mu_0 \dfrac{\partial \boldsymbol{H}}{\partial t} \\ \boldsymbol{\nabla} \times \boldsymbol{H} = \varepsilon_0 \dfrac{\partial \boldsymbol{E}}{\partial t} \end{cases} \tag{1}$$

Here, μ_0 and ε_0 are dielectric constant and permeability in vacuum, respectively. From equation (1), we have the explicit representation of electromagnetic field $\boldsymbol{E}$ and $\boldsymbol{B}$ in a spherical coordinate system. It is known that there exists a solution for that electro field or magnetic field cirques around the near surface of a sphere. In case of this solution, the intensity of scattered light and internal transmitted light is enlarged and strong resonance phenomena occurs. This resonance in a sphere is the WGM resonance.

WGM resonance only occurs for limited values of incident wavelengths. Frankly speaking, WGM resonance occurs only when the circumference of the sphere nearly equals to some integer multiplication of the incident wavelengths like the Bohr's quantum condition. WGM resonance is known as the resonance phenomena with high Q-value, i.e. if the incident wavelengths slightly changed the scattered and transmitted intensity clearly decreases. Compared with the Fabry-Pèrot interferometer, which is known as high Q-valued resonator (10^5~10^8)[2], Q-value of WGM resonator can be 10^7~10^9 in one exemplary aspect[3].

These WGM resonant wavelengths are determined from the equation called the dispersion equation of a sphere. The dispersion equation is derived from the exact solution of the Maxwell's equation (i.e. Mie scattering theory) without any kinds of approximation.

The dispersion equation of a sphere for TE / TM modes are given as follows.

$$\frac{\mu_1}{n_1^2 j_l(\rho_1)} \frac{\partial[\rho_1 j_l(\rho_1)]}{\partial \rho_1} = \frac{\mu_0}{n_0^2 h_l^{(1)}(\rho_0)} \frac{\partial\left[\rho_0 h_l^{(1)}(\rho_0)\right]}{\partial \rho_0} \qquad \text{for TE mode} \tag{2}$$

$$\frac{1}{\mu_1 j_l(\rho_1)} \frac{\partial[\rho_1 j_l(\rho_1)]}{\partial \rho_1} = \frac{1}{\mu_0 h_l^{(1)}(\rho_0)} \frac{\partial\left[\rho_0 h_l^{(1)}(\rho_0)\right]}{\partial \rho_0} \qquad \text{for TM mode} \tag{3}$$

where, j_l, $h_l^{(1)}$ denote the spherical Bessel function and the first spherical Hankel function of order l (angular mode number), respectively. We use the following notation through this article: the lower subscript 0 means that the parameter is about the surrounding air, whereas the lower subscript 1 means the parameter is about inside of the object cavity. Based on this notation, $\rho_{0,1} = k_{0,1} a$, where n denotes refractive index, k denotes the wave number. As stated above, the dispersion equation of a sphere is the strict result without any kind of approximation, and numerical solutions of equation (2) or (3) can be easily obtained. But it is sometimes useful to have other forms of equations for determining WGM resonant wavelengths by using finite

power series expansion approximation. Expanding the dispersion equation by using Airy functions, we get another representation of equation (2) or (3) as follows[4].

$$\lambda = 2\pi an\left[l+\frac{1}{2}-\alpha_1\left(\frac{l+\frac{1}{2}}{2}\right)^{\frac{1}{3}}-\frac{\chi n}{\sqrt{n^2-1}}+\frac{3\alpha_q^2}{2^{\frac{2}{3}}10\left(l+\frac{1}{2}\right)^{\frac{1}{3}}}-\frac{\chi n^3(2\chi^2-3)\alpha_q}{3\cdot 2^{\frac{1}{3}}(n^2-1)^{\frac{3}{2}}\left(l+\frac{1}{2}\right)^{\frac{2}{3}}}\right]^{-1} \quad (4)$$

where a denotes the radius of the sphere, α_q denotes the qth zero point of Airy functions, q denotes the radial mode number χ characterizes the polarization mode: $\chi = 1$ for TE mode and $1/n_1^2$ for TM mode. When model parameters (refractive index and radius of a sphere) and angular mode number l are given, equation (2) or (3) has several solutions. In other words, corresponding to one given condition, a family of WGM resonant wavelengths $\{\lambda_{l,q}\}_{q\in\mathbb{N}}(\lambda_{l,1} > \lambda_{l,2} > \cdots)$ are calculated from (4). These ordered number q corresponds to radial mode number of WGM resonance. From the representation (4), we can directly calculate the WGM resonant wavelengths for each mode numbers. It is remarkable that azimuthal mode number m does not exist in equation (4). This suggests that all different azimuthal modes degenerate because of a rotational symmetry of a perfect sphere. This approximation requires that the radius of the measurement object is much larger than the wavelength range, i.e., $a \gg \lambda_0$ is true[4].
In **Table.3**, Numerical examples of WGM resonant wavelengths are shown.

Table.3 Validity of approximate expansion (4) for several condition (polar mode: TE mode, refractive index of a sphere: 1.5). λ_1: WGM resonant wavelengths calculated from dispersion equation (2). λ_2: WGM resonant wavelengths calculated from approximate expansion (4)

radius of sphere[μm] (angular mode number)	λ_1 [nm]	λ_2 [nm]	$\Delta\lambda = \lambda_1 - \lambda_2$ [nm]
10(l=54)	1561.6073	1561.3543	0.2530
10(l=55)	1535.0870	1534.8497	0.2373
10(l=56)	1509.4651	1509.2422	0.2229
50(l=289)	1567.8904	1567.8864	0.0040
50(l=290)	1562.6177	1562.6144	0.0033
50(l=291)	1557.3817	1557.3780	0.0037
50(l=292)	1552.1798	1552.1767	0.0032
50(l=293)	1547.0139	1547.0102	0.0037
50(l=294)	1541.8814	1541.8781	0.0033
50(l=295)	1536.7830	1536.7801	0.0029
50(l=296)	1531.7193	1531.7159	0.0034
50(l=297)	1526.6880	1526.6851	0.0029
50(l=298)	1521.6906	1521.6874	0.0032
100(l=586)	1568.7199	1568.7197	0.0001
100(l=587)	1566.0910	1566.0902	0.0008
100(l=588)	1563.4694	1563.4694	0.0000
100(l=589)	1560.8581	1560.8574	0.0006
100(l=590)	1558.2540	1558.2542	0.0002
100(l=591)	1555.6601	1555.6597	0.0004
100(l=592)	1553.0743	1553.0738	0.0005
100(l=593)	1550.4966	1550.4965	0.0001
100(l=594)	1547.9280	1547.9278	0.0002
100(l=595)	1545.3683	1545.3676	0.0007
100(l=596)	1542.8166	1542.8159	0.0007
100(l=597)	1540.2728	1540.2726	0.0002
100(l=598)	1537.7378	1537.7377	0.0001
100(l=599)	1535.2117	1535.2112	0.0005
100(l=600)	1532.6933	1532.6930	0.0004
100(l=601)	1530.1837	1530.1830	0.0007

2.3 Diameter measurement based on WGM resonance

In this section, how to measure the sphere-diameter based on WGM resonance will be briefly described. As stated in introduction, a comprehensive purpose of this research is measuring sphere diameter based on WGM resonance. For its high Q-value over 10^7, say, WGM resonance occurs only for discrete values of incident wavelengths. If the radius of the object sphere is known, these particular WGM resonant wavelengths are determined in advance by theoretical calculus, i.e. by solving the dispersion equation of a sphere. On an experimental aspect, we transmit stationary incident light wave from one side of an optical fiber with its wavelengths continuously changed and measure the transmitted spectrum on the other side of the fiber. When the light wave with WGM resonant wavelength is projected, a great deal of transmitted intensity clearly vanishes. Hence, the WGM resonant wavelengths are precisely measured experimentally. On the other hand, as stated above, values of WGM resonant wavelengths are deterministic by the Mie scattering theory: the dispersion equation predicts all values theoretically. So, by fitting experimentally measured values and theoretically calculated values, the unknown value of the radius of the sphere is estimated. This is the major principle of the measurement method based on WGM resonance.

3. THEORETICAL BACKGROUND AROUND SPHEROIDAL DISTORTION

3.1 Spheroidal distortion

In the measurement method described above, the measurement object supposed to be a perfect sphere. In other words, this measurement method does not correspond to the case that the measured object has some distortion. However, it is often the case that the measured object is not a perfect sphere. It sometimes contains some distortion like following: chipped or dazzling in micro scale, or flatly crushed or elongated in macro scale. Here, we will explain how these kinds of distortion affects the measurement result.

Now suppose that the same incident light is repeatedly projected from several directions. When the object is a perfect sphere, the measured transmitted light spectrum is invariant since a perfect sphere geometrically has a rotational symmetry. On one exemplary aspect, however, if the object sphere is elongated to spheroidal shape, resonant wavelengths varies corresponding to the propagating direction. In this case, a degeneracy for azimuthal direction disappears, i.e., different azimuthal mode numbers corresponds to different WGM resonant wavelengths. **Fig.4** shows the conceptual diagram of such disappearance of degeneracy along azimuthal direction.

As stated above, many kinds of distortion from a perfect sphere can be considered. Among these kinds of distortion, spheroidal distortion is the essential distortion while considering the macro distortion. This is because a distorted sphere still has a rotational symmetry. Many of micro-sphere particles are made based on the concentration property of the constituent: they are manufactured by using surface tension, which is dominant to a micro particle. Hence, even a sphere particle distorted by some remote field strength such as a gravity, it still has a rotational symmetry and an important part of its scattering property would be explained by a spheroidal model. By that meaning, above kind of distortion is an essential example in evaluating the distortion from a perfect sphere.

From a viewpoint of above consideration, our aim is to expand the model from a perfect sphere to a spheroid. In this article, as also stated in introduction, we propose a measurement method to evaluate the spheroidal distortion. Details of the measurement strategy will be described in following sections.

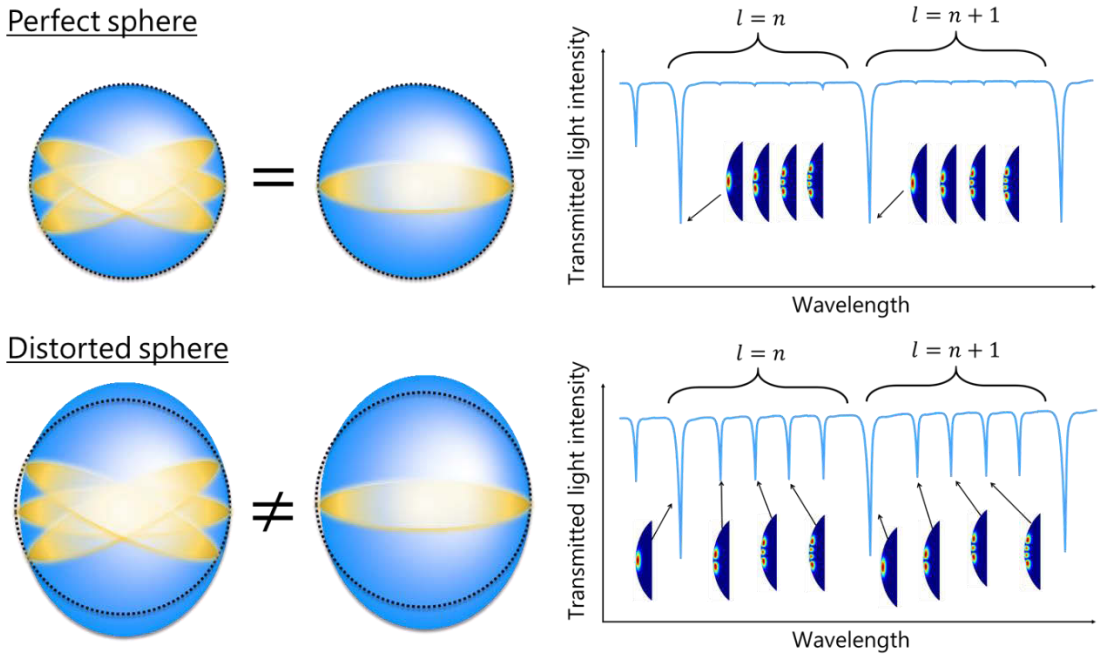

Fig.4 Transmitted light spectrum for the case that the object has spheroidal distortion

3.2 General consideration

In this section, we explain the theoretical background about solving the interaction problems between light wave and spheroidal particles. Spheroids are generated by rotating a plane ellipse and there are two kinds of spheroids: rotation about the longer axis generates a prolate spheroid, whereas rotation about the shorter axis generates an oblate spheroid. When one treats spheroidal particles, spheroidal coordinate system is always appropriate for analysis of physical phenomena relating to spheroidal particles. The coordinate transformation formula between the Cartesian coordinate (x, y, z) and spheroidal coordinate system (ξ, η, ϕ) is following.

$$\begin{cases} x = l\sqrt{1-\eta^2}\sqrt{\xi^2 \pm 1}\,cos\,\phi \\ y = l\sqrt{1-\eta^2}\sqrt{\xi^2 \pm 1}\,sin\,\phi \\ z = \quad l\xi\eta \end{cases} \tag{6}$$

for prolate: $-1 \le \eta \le 1, 1 \le \xi < \infty, 0 \le \phi \le 2\pi$

for oblate: $-1 \le \eta \le 1, 0 \le \xi < \infty, 0 \le \phi \le 2\pi$

Here, l denotes the semi-focal distance of the spheroid and parameter ξ represents how large the particle spread, whereas the parameter η represents how the spheroidal object is elongated (for prolate) or flattened (for oblate). In spheroidal coordinate systems, a position of an arbitrary point is denoted by (ξ, η, ϕ) (**Fig.5**).

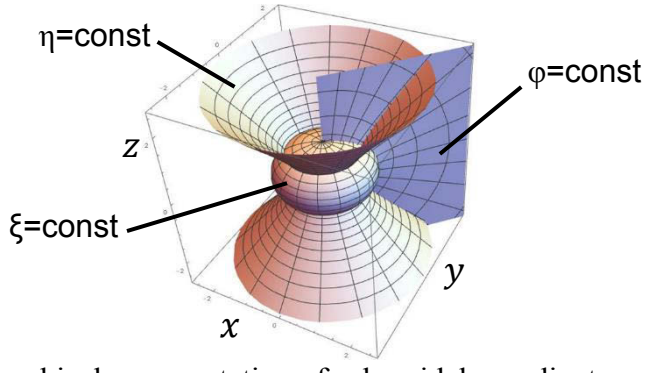

Fig.5 Graphical representation of spheroidal coordinate systems

Ideally, it is desirable to solve the Maxwell's equations in spheroidal coordinate system based on separation of variables method (SVM) as same as the spherical case and know the WGM resonant wavelengths for spheroidal particles theoretically. In other words, the dispersion equation for spheroidal particle is more necessary than anything so far as we stand on the same perspective as the spherical case. However, in view of measuring a spheroidal particle, this approach is not appropriate by following reason: in this case, Maxwell's equations can be solved in the separation of variable method in a classical meaning[5], but the representation of the solution is too complex to treat easily even on numerical calculation. In particular, the electromagnetic field in the system will be explicitly represented as an infinite power series of the spheroidal wave functions, but the speed of convergence is extremely slow and yet the convergence of the expansion is not proved mathematically. If we tried to obtain the explicit formula of the dispersion equation of spheroid, the representation should be the form "the determinant of infinite dimensional matrix is zero" as following:

$$det\begin{pmatrix} \mathfrak{S}^0_{m,m} & \mathfrak{S}^0_{m,m+1} & \mathfrak{S}^0_{m,m+2} & \\ \mathfrak{S}^1_{m,m} & \mathfrak{S}^1_{m,m+1} & \mathfrak{S}^1_{m,m+2} & \cdots \\ \mathfrak{S}^2_{m,m} & \mathfrak{S}^2_{m,m+1} & \mathfrak{S}^2_{m,m+2} & \\ & \vdots & & \ddots \end{pmatrix} = 0 \tag{7}$$

Here, each component is expressed as following.

$$\mathfrak{S}^t_{m,n} = i^n \begin{pmatrix} V^{(3),t}_{mn}(c_0) & U^{(3),t}_{mn}(c_0) & -V^{(1),t}_{mn}(c_1) & -U^{(1),t}_{mn}(c_1) \\ Y^{(3),t}_{mn}(c_0) & X^{(3),t}_{mn}(c_0) & -Y^{(1),t}_{mn}(c_1) & -X^{(1),t}_{mn}(c_1) \\ U^{(3),t}_{mn}(c_0) & V^{(3),t}_{mn}(c_0) & -\mathcal{H}U^{(1),t}_{mn}(c_1) & -\mathcal{H}V^{(1),t}_{mn}(c_1) \\ X^{(3),t}_{mn}(c_0) & Y^{(3),t}_{mn}(c_0) & -\mathcal{H}X^{(1),t}_{mn}(c_1) & -\mathcal{H}Y^{(1),t}_{mn}(c_1) \end{pmatrix} \tag{8}$$

Each component of matrix (8) is a function of wavelengths and parameters about the model (the concrete representation of each component is showed in **APPENDIX**). The representation form (7) is so complicated that it is difficult to solve it even numerically. Generally, it is still difficult to solve the wave equation in an arbitrary coordinate system (that is more complicated than the spherical coordinate system) and obtain the explicit solution in the classical forms. Hence, we are forced to use some approximation enough not to miss the physical characteristics.

3.3 Approximate representation of WGM resonant wavelengths of a spheroid.

We use an approximate representation formula of WGM resonant wavelengths for spheroids. How the approximation method was used for deriving the representation will be briefly described. When we try to derive the classical solution of Maxwell's equations in spheroidal coordinate systems, consider the Helmholtz equation (namely, scalar wave equation of three dimension):

$$\Delta\Phi + k^2\Phi = 0 \tag{9}$$

where Δ is the Laplacian in spheroidal coordinate systems, and Φ is the scalar potential. In the separation of variables method, a solution $\Phi(\xi,\eta,\phi) = X(\xi)Y(\eta)Z(\phi)$ is found but the explicit representation of that solution is too complex to treat well. Hence, now we only focus on a solution of straight rays

$$\Phi(\boldsymbol{r}) = A(\boldsymbol{r})\, exp\big(ik_0 S(\boldsymbol{r})\big). \tag{10}$$

The first order approximation for the phase function S, called eikonal, is determined by the eikonal equation:

$$|\nabla S(\boldsymbol{r})|^2 = \varepsilon(\boldsymbol{r}) \tag{11}$$

where $\varepsilon(\boldsymbol{r})$ is the optical susceptibility: equals to n_1^2 inside the cavity and equals to $n_0^2 = 1$ outside the cavity. As following expansion shows, in the range that geometrical optics approximation holds, it suffices to use the eikonal solution of Maxwell's equation to know

WGM resonant wavelengths in a spheroid. By Gorodetsky et al., the approximate formula of the WGM resonant wavelengths of spheroid should be[6]:

$$\lambda_p = 2\pi an\left[l - \alpha_q\left(\frac{l}{2}\right)^{\frac{1}{3}} + \frac{2p(a-b)+a}{2b} - \frac{\chi n}{\sqrt{n^2-1}} + \frac{3\alpha_q^2}{20}\left(\frac{l}{2}\right)^{-\frac{1}{3}} - \frac{\alpha_q}{12}\left(\frac{2p(a^3-b^3)+a^3}{b^3} + \frac{2n\chi(2\chi^2-3n^2)}{(n^2-1)^{\frac{3}{2}}}\right)\left(\frac{l}{2}\right)^{-\frac{2}{3}} + O(l^{-1})\right]^{-1} \quad (12)$$

where α_q is a q th zero point of the Airy function and $\chi = 1$ for TE mode and $1/n_1^2$ for TM mode. A integer $p = l - |m|(p = 0,1,\dots,l)$ denotes the azimuthal direction for every fixed angular mode number l. Here we write the lower subscript p to emphasize that resonant wavelengths also depend on azimuthal propagation direction.

Hereafter we verify the values of resonant wavelengths calculated from equation (12) is consistent in particular spectrum range. Above approximation by restriction of the solutions is based on geometrical optics. It is known that eikonal approximation is credible when the length of the optical paths is much larger than the wavelength. This circumstance is same as the case of the expansion of the dispersion equation of a sphere (expansion (4)). **Fig.6** shows the difference between the two distinct values of WGM resonant wavelengths: one is calculated from the expansion (4), whereas the other is calculated by the expansion (12) when let the shorter axis radius a be equal to the longer axis radius b (here assumed that the radius of the sphere is 100 μm and the refractive index is constant 1.5). This shows that, when the measured object is a perfect sphere, two distinct values of resonant wavelengths calculated from expansion (4) and (12) varies in order of 10^{-11} and the expansion (12) is consistent when the model is a perfect sphere in this order.

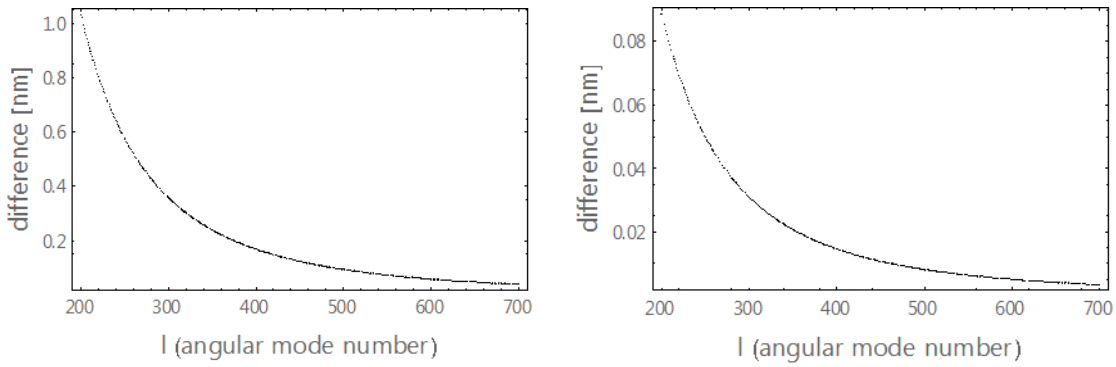

Fig.6 WGM resonant wavelengths for spheroidal distortion

4. PROPOSAL OF THE MEASUREMENT STRATEGY TO EVALUATE THE DEGREE OF SPHEROIDAL DISTORTION OF THE PARTICLE

4.1 Non-degeneracy along azimuthal direction and spheroidal distortion

As stated repeatedly, our purpose is to evaluate the spheroidal distortion of the object sphere. To achieve this, we focus on the geometrical characteristic of spheroids that both prolate and oblate spheroids do not have the rotational symmetry except for about the rotational axis. From this fact, optical path lengths differs depending on a propagating direction of light wave. In short, for a spheroid, the degeneracy along azimuthal direction disappears.

To see this, let the object be a prolate spheroid and assume that the incident light wave projected perpendicular to the rotational axis. For simplicity, hereafter, we consider only prolate spheroids. In this case, while the fundamental mode that light wave oscillates in equatorial plane of the spheroid is excited, other modes that light wave propagates in spread area along azimuthal

direction are excited at the same time. It is intuitively clear from the geometrical characteristic of a prolate spheroid that the optical path for the latter mode has the longer lengths than for the former one. Azimuthal mode number suggests that how wide the propagating light spreads along the azimuthal direction. As same as the case for a perfect sphere (shown in **Fig.2**), large azimuthal mode number corresponds to the propagation mode such that the light wave spreads widely from the equatorial plane. Hence, prolate-spheroidal shape comprises the following property: the larger the azimuthal mode number, the longer the optical path lengths.

Now we describe in detail the above intuitive discussion by using expansion (10). In **Fig.7**, WGM resonant wavelengths for a prolate spheroid (whose refractive index is 1.5 and shorter axis lengths is 100 μm) for several azimuthal mode numbers are plotted as explicit functions of degree of spheroidal distortion b/a. The upper graph is an enlarged view of the lower one. Here, let the radial mode number is consistently 1, and the graphs for azimuthal mode number $p = 0,1,2,3,4,5$ (i.e. for $m = l, \dots, l-5$) are plotted. As obvious from the fact that the values of optical path length for large azimuthal mode number monotone increase about the azimuthal mode number (consequently, whose WGM resonant wavelengths also increase), six curves in **Fig.7** corresponds to $p = 0,1,2,3,4,5$ in order from the smaller-valued curve.

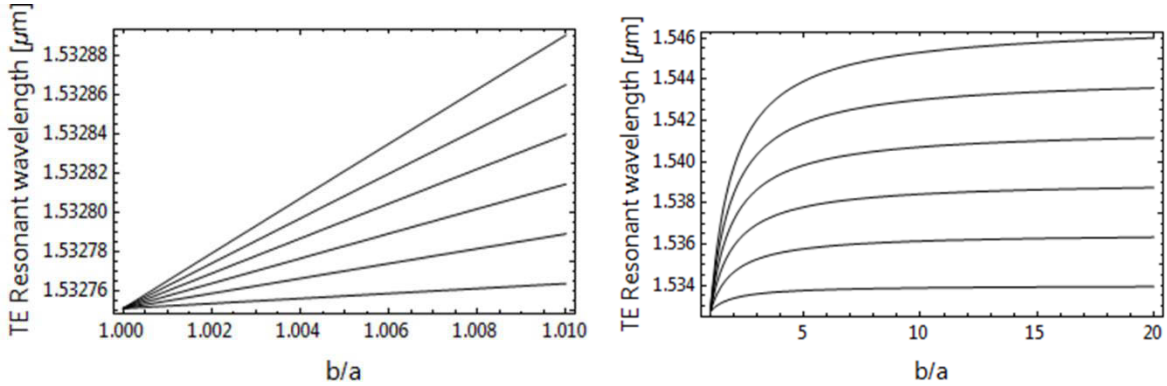

Fig.7 WGM resonant wavelengths for spheroidal distortion (light graph is the enlarged view of right graph)

4.2 Proposal of measurement strategy

In this section, we propose a new measurement method to evaluate the degree of spheroidal distortion of the particle. First, as the upper graph of **Fig.8** suggests, values of WGM resonant wavelengths linearly increase about the degree of spheroidal distortion b/a if it is close to 1. Consequently, regarding the upper graph consists of several lines, the degree of variation among wavelengths pitches for each azimuthal mode number of one by one is small. To see this, we calculate a relative standard deviation of wavelengths pitches as a function of the degree of spheroidal distortion b/a in the following meaning. Let $\Omega = \{\omega_1, \dots, \omega_l\}$, $\mathcal{F} = 2^{\Omega}$ and $\mathbb{P}$ be a discrete probability measure. On this probability space $(\Omega, \mathcal{F}, \mathbb{P})$, define a random variable $\Delta\lambda: \Omega \to \mathbb{R}$ by $\Delta\lambda(\omega_p) = \lambda_p - \lambda_{p-1}$ $(p = 1,2, \dots, l)$. Then define dimensionless quantity RSD (relative standard deviation) by:

$$RSD = \frac{\sqrt{Var[\Delta\lambda]}}{E[\Delta\lambda]} \tag{13}$$

Fig.8 plots this values as a function of the degree of spheroidal distortion b/a. Here, the model is the same as in section 4.1 (prolate spheroid whose refractive index is 1.5, shorter axis radius is 100 μm). The polarization mode is TE mode and let $l = 600$, $q = 1$.

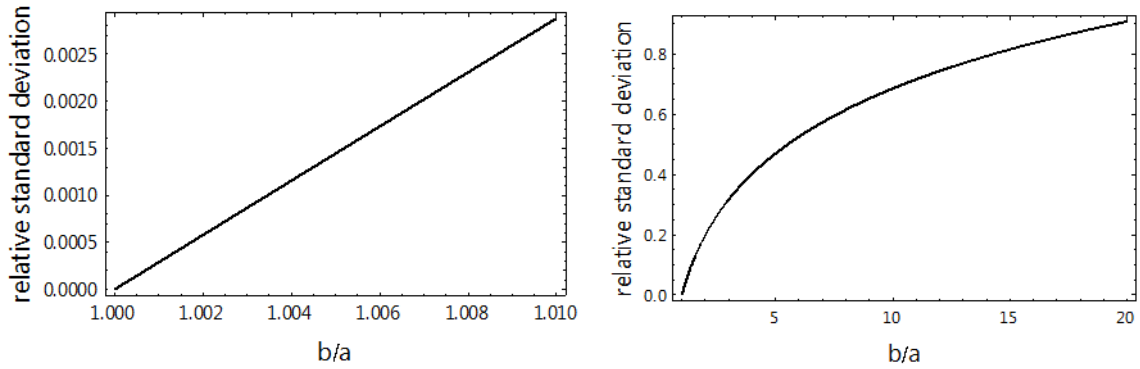

Fig.8 relative standard deviation of Δλ
(light graph is the enlarged view of right graph)

This shows that the WGM resonant wavelengths pitches are invariant regardless of azimuthal mode numbers. Hence, several peaks that appeared in case of prolate spheroids are explained by the non-degeneracy along azimuthal mode direction. In addition, the pitches between each 'sub-peaks' are regarded as constant if the degree of prolate-spheroidal distortion b/a is close to 1.

Now we propose a way to evaluate the degree of spheroidal distortion using these pitch values with respect to azimuthal mode numbers. From the transmitted light wave spectrum, pitches $\Delta\lambda$ are measured so that the degree of spheroidal distortion can be evaluated from these values as follows. First, assume that there is ideally no experimental restriction and all values of pitches corresponding to $p = 0,1, \dots, l$ can be measured precisely. Let $\{\widehat{\Delta\lambda_p}\}_{p=1,2,\dots,l}$ be experimentally measured several values of pitches between different azimuthal mode numbers next to each other. Then, the degree of spheroidal distortion b/a can be estimated from following several equations based on the expansion (12):

$$\begin{cases} \widehat{\Delta\lambda_1} = \lambda_1 - \lambda_0 \\ \widehat{\Delta\lambda_2} = \lambda_2 - \lambda_1 \\ \quad\vdots \\ \widehat{\Delta\lambda_l} = \lambda_l - \lambda_{l-1} \end{cases} \tag{14}$$

Actually, there is a difficulty on realizing the above method. Since on circumstance that the shorter axis radius of the model is unknown and we can use only the information of resonant wavelengths, it is experimentally hard to detect the azimuthal mode numbers corresponding to the measured resonant wavelengths. Also, it is often the case that we can use only subsequence of the measured wavelengths values (i.e. whose number of values is fewer than l). So, if we conduct the above evaluation strategy in an experimental setup, following strategy should be applied. Let $\{\widehat{\Delta\lambda_p}\}_{p=1,2,\dots,l_0}(l_0 \le l)$ be a sequence of l_0 credible values of measured wavelengths pitches between different azimuthal mode numbers next to each other. Then take an expectation of these values $\widehat{\Delta\lambda} = \frac{1}{l_0}\left(\widehat{\Delta\lambda_1} + \cdots + \widehat{\Delta\lambda_{l_0}}\right)$ and the degree of spheroidal distortion b/a can be estimated by

$$\widehat{\Delta\lambda} = E[\Delta\lambda] = \int_\Omega \Delta\lambda(\omega)\mathbb{P}(d\omega)\left(= \frac{1}{l}\sum_{1\le p\le l}\Delta\lambda(\omega_p)\right) \tag{15}$$

This averaging procedure is justified because of the invariance of pitches for each azimuthal modes stated at the beginning of this section.

4.3 Discussion

We suggested the measurement strategy to evaluate the degree of prolate-spheroidal distortion. In section 4.2, we stated that there is an experimental restriction that azimuthal mode numbers cannot be detected. In addition to this, there are some other experimental restriction. First, the measurement accuracy of WGM resonant wavelengths depends on the performance of the spectrometer. In other words, if the pitches of resonant wavelengths corresponding to different azimuthal mode numbers next to each other are smaller than the resolution of the spectrometer cannot be discriminated so that there is no knowing about precise values of pitches. So, for each value of resolution, there exists a minimal value of distortion for which we can measure pitches between different azimuthal mode numbers next to each other. For example, if the shorter axis radius is 100 μm and the resolution of the spectrometer is 0.1nm, then the minimal value of degree of spheroidal distortion is 1.0377. in other words, if the measured spheroidal object is distorted over 1.0377 (i.e. $b \geq 1.0377a$ holds), then the distortion can be detected experimentally. **Table.9** shows the several numerical exemplary values of minimal degree of prolate-spheroidal distortion which can be measured when the resolution of the spectrometer is 0.1 nm.

Table.9 Degree of prolate-spheroidal distortion which can be measured if the resolution of the spectrometer is 0.1 nm (refractive index is 1.5 and radial mode number q is 1).

Short radius of the spheroid [μm]	Angular mode number (corresponding resonant wavelength when b/a is 1 [μm])	Measurable minimal spheroidal distortion
1	10 (1.35861)	1.00031
50	300 (1.51244)	1.01942
100	600 (1.53305)	1.0377
500	3000 (1.55742)	1.16548
1000	6000 (1.56229)	1.29667

CONCLUSIONS

In this study, we proposed a new measurement method for which the degree of spheroidal distortion of the object sphere can be evaluated. This method uses WGM resonant wavelengths for each azimuthal mode based on the disappearance of the degeneracy for the azimuthal direction for a spheroidal particle. We also appreciated the validity of this measurement method.

APPENDIX

Here we show the concrete representation of components appeared in matrix (7).

$$U_{mn}^{(j),t}(c_{1,0}) = m\xi_0 R_{mn}^{(j)}(c_{1,0};\xi_0)[(\xi_0^2-1)B_t^{mn}(c_{1,0}) + 2(\xi_0^2-1)A_t^{mn}(c_{1,0}) + E_t^{mn}(c_{1,0})] \quad \text{(A.1)}$$

$$V_{mn}^{(j),t}(c_{1,0}) = \frac{i}{c_{1,0}}\Bigg\{\frac{m^2 R_{mn}^{(j)}(c_{1,0};\xi_0)}{\xi_0^2-1}\left[(\xi_0^2-1)^2 D_t^{mn}(c_{1,0}) + 2(\xi_0^2-1)C_t^{mn}(c_{1,0}) + F_t^{mn}(c_{1,0})\right] - R_{mn}^{(j)}(c_{1,0};\xi_0^2)\left[\lambda_{mn}(c_{1,0}) - (c_{1,0}\xi_0)^2 + \frac{m^2}{\xi_0^2-1}\right]\left[(\xi_0^2-1)C_t^{mn}(c_{1,0}) + F_t^{mn}(c_{1,0})\right] + \xi_0(\xi_0^2-1)\left[\frac{dR_{mn}^{(j)}(c_{1,0};\xi)}{d\xi}\right]_{\xi_0}\left[2C_t^{mn}(c_{1,0})\xi_0 + (\xi_0^2-1)G_t^{mn}(c_{1,0}) + I_t^{mn}(c_{1,0})\right] + R_{mn}^{(j)}(c_{1,0};\xi_0)\left[(\xi_0^2-1)^2 G_t^{mn}(c_{1,0}) + (3\xi_0^2-1)I_t^{mn}(c_{1,0})\right]\Bigg\} \tag{A.2}$$

$$X_{mn}^{(j),t}(c_{1,0}) = \xi_0 R_{mn}^{(j)}(c_{1,0};\xi_0)G_t^{mn}(c_{1,0}) - \left[\frac{dR_{mn}^{(j)}(c_{1,0};\xi)}{d\xi}\right]_{\xi_0} C_t^{mn}(c_{1,0}) \tag{A.3}$$

$$Y_{mn}^{(j),t}(c_{1,0}) = \frac{i}{c_{1,0}} m\left(\frac{1}{\xi_0^2-1}R_{mn}^{(j)}(c_{1,0};\xi_0)\left[A_t^{mn}(c_{1,0}) + H_t^{mn}(c_{1,0})\right] + \left\{R_{mn}^{(j)}(c_{1,0};\xi_0) + \xi_0\left[\frac{dR_{mn}^{(j)}(c_{1,0};\xi)}{d\xi}\right]_{\xi_0}\right\}B_t^{mn}(c_{1,0})\right) \tag{A.4}$$

Here, $c_{1,0} = l \cdot k_{0,1}$, closed curve $\xi = \xi_0$ denotes the surface of the object spheroid and $R_{mn}^{(j)}(c_{1,0};\xi_0)$ is the radial spheroidal wave function where upper subscript *j* classifies the asymptotic behavior of the radial spheroidal wave function as follows:

$$R_{mn}^{(1)} \to \frac{1}{c\xi}cos\left(c\xi - \frac{n+1}{2}\pi\right) \tag{A.5}$$

$$R_{mn}^{(2)} \to \frac{1}{c\xi}sin\left(c\xi - \frac{n+1}{2}\pi\right) \tag{A.6}$$

$$R_{mn}^{(3)} \to \frac{1}{c\xi}exp\left[i\left(c\xi - \frac{n+1}{2}\pi\right)\right] \tag{A.7}$$

$$R_{mn}^{(4)} \to \frac{1}{c\xi}exp\left[-i\left(c\xi - \frac{n+1}{2}\pi\right)\right] \tag{A.8}$$

Also, $A_t^{mn}, B_t^{mn}, C_t^{mn}, D_t^{mn}, E_t^{mn}, F_t^{mn}, G_t^{mn}, H_t^{mn}, I_t^{mn}$ are defines as expansion coefficients of following functions of angular spheroidal wave function $S_{mn}(\eta)$ by associated Legendre function $P_m^n(\eta)$:

$$(1-\eta^2)^{1/2}S_{mn}(\eta) = \sum_{t=0}^{\infty} A_t^{mn} \cdot P_{m-1+t}^{m-1}(\eta) \tag{A.9}$$

$$(1-\eta^2)^{-1/2}S_{mn}(\eta) = \sum_{t=0}^{\infty} B_t^{mn} \cdot P_{m-1+t}^{m-1}(\eta) \tag{A.10}$$

$$\eta(1-\eta^2)^{1/2}S_{mn}(\eta) = \sum_{t=0}^{\infty} C_t^{mn} \cdot P_{m-1+t}^{m-1}(\eta) \quad \text{(A.11)}$$

$$\eta(1-\eta^2)^{-1/2}S_{mn}(\eta) = \sum_{t=0}^{\infty} D_t^{mn} \cdot P_{m-1+t}^{m-1}(\eta) \quad \text{(A.12)}$$

$$(1-\eta^2)^{3/2}S_{mn}(\eta) = \sum_{t=0}^{\infty} E_t^{mn} \cdot P_{m-1+t}^{m-1}(\eta) \quad \text{(A.13)}$$

$$\eta(1-\eta^2)^{3/2}S_{mn}(\eta) = \sum_{t=0}^{\infty} F_t^{mn} \cdot P_{m-1+t}^{m-1}(\eta) \quad \text{(A.14)}$$

$$(1-\eta^2)^{1/2}\frac{dS_{mn}(\eta)}{d\eta} = \sum_{t=0}^{\infty} G_t^{mn} \cdot P_{m-1+t}^{m-1}(\eta) \quad \text{(A.15)}$$

$$\eta(1-\eta^2)^{1/2}\frac{dS_{mn}(\eta)}{d\eta} = \sum_{t=0}^{\infty} H_t^{mn} \cdot P_{m-1+t}^{m-1}(\eta) \quad \text{(A.16)}$$

$$(1-\eta^2)^{3/2}\frac{dS_{mn}(\eta)}{d\eta} = \sum_{t=0}^{\infty} I_t^{mn} \cdot P_{m-1+t}^{m-1}(\eta) \quad \text{(A.17)}$$

ACKNOWLEDGEMENT

This study was supported by JSPS Grant-in-Aid for Scientific Research (KAKENHI) (Grant No. 15H05505) and Mizuho Foundation for the Promotion of Sciences.

REFERENCES

[1] M. Michihata, T. Hayashi, A. Adachi, and Y. Takaya: "Measurement of probe- stylus sphere diameter for micro-CMM based on spectral fingerprint of whispering gallery modes," CIRP Annals, Manufacturing Technology, **63**, pp. 469-472 (2014).

[2] Y. Akahane, T. Asano, B. S. Song, and S. Noda: "High-Q photonic nanocavity in a two-dimensional photonic crystal," Nature, vol.425, pp. 944-947 (2003).

[3] A. Chiesera, Y. Dumeige, P. Fèron, M. Ferrari, Y. Jestin, G. N. Conti, S. Pelli, S. Soria, and G. C. Righimi: "Spherical whispering-gallery-mode microresonators," Laser&Photon. Rev, vol.4, **3**, pp.457-482 (2010).

[4] S. Schiller, and R. L. Byer: "High-resolution spectroscopy of whispering gallery modes in large dielectric sphere," Opt. Letters, vol.16, **15**, pp. 1138-1140 (1991).

[5] S. Asano, and G. Yamamoto: "Light scattering by a spheroidal particle," Appl. Opt., vol.14, **1**, pp. 29-49 (1975).

[6] M. L. Gorodetsky, and A. E. Fomin: "Geometrical theory of whispering gallery modes," IEEE journal of selected topics in quantum electronics, vol. 12, **1**, pp. 33-39 (2006).

CONTACTS

K. Hayashi hayashi.k@nanolab.t.u-tokyo.ac.jp
Dr. M. Michihata michihata@nanolab.t.u-tokyo.ac.jp